Thermal counterflow experiments on superfluid helium at temperatures close to T_λ

A. G. F. Dorscheidt,* H. van Kempen, and P. Wyder
Research Institute for Materials, University of Nijmegen, Toernooiveld, 6525 ED Nijmegen, The Netherlands

T. H. K. Frederking
University of California at Los Angeles, Los Angeles, California 90024
(Received 11 January 1985)

We have studied the relation between the heat-current density W and the temperature gradient ∇T in the laminar, turbulent, and transition regions in superfluid helium for temperatures close to T_λ in channels of circular cross section. For temperatures $T_\lambda - T < 0.05$ K, we do find simple exponentional relationships. In the turbulent region, $W/\nabla T$ is independent of channel diameter and is proportional to $(T_\lambda - T)^{0.85}$. The critical heat flow W_c is proportional to $(T_\lambda - T)^\beta$ with $\beta = -0.75 \pm 0.05$. For the diameter (d) dependence of W_c, we found $W_c \propto d^\nu$, with $\nu = -0.80 \pm 0.03$. The transition from the linear region to the turbulent region is very steep but not discontinuous. In the transition region the characteristic times related to the buildup of the turbulence become extremely long, especially for the narrowest channel and for T close to T_λ.

I. INTRODUCTION

Heat-conductivity measurements in superfluid helium typically show the existence of two heat-current-density regions: the subcritical region and the supercritical region, separated by an intermediate region (the critical-heat-current-density region). The heat conductivity in the subcritical region can be described in terms of a two-fluid model as a pure laminar-counterflow mechanism. This leads to the linear London-Zilsel relation,[1] which for circular flow channels takes the form

$$\nabla T = \frac{32\eta W}{d^2(\rho S)^2 T} . \tag{1}$$

Here, ∇T is the temperature gradient, W is the heat-current density, η is the viscosity, ρ is the total fluid density composed as $\rho = \rho_n + \rho_s$, where ρ_n and ρ_s are the density of the normal and superfluid component, respectively, d is the channel diameter, and S is the entropy. The supercritical, or turbulent, phase is commonly described by introducing a mutual friction force which leads to the generalized Gorter-Mellink expression

$$\nabla T = \frac{A\rho_n}{S}\left[\frac{W}{\rho_s S T}\right]^m . \tag{2}$$

The exponent m in this expression is usually found to be 3,[2] but it has the tendency to increase when T_λ is approached.[3] A is a temperature-dependent factor. A more thorough theoretical treatment on turbulence in helium is given by Vinen[4] and Schwarz.[5] The critical heat-current density W_c, which separates the two heat-transport regions, leads, in the two-fluid model, to a critical superfluid velocity

$$v_{sc} = \frac{\rho_n W_c}{\rho\rho_s S T} . \tag{3}$$

Experimental results on the critical velocity and critical-heat-current density at temperatures close to T_λ have been scarce until now because of sensitivity problems encountered in measuring the very small temperature differences involved. Additionally, temperature-control problems become more severe when one approaches T_λ because of the extremely fast varying thermal properties.

In this paper we describe experiments which investigate the critical-heat-current region for temperatures close to T_λ. In this temperature range it is difficult to obtain a complete picture by performing measurements on one channel. Therefore, to get a complete picture, we used capillaries with three different diameters. The smallest-diameter capillary, called channel I hereafter, shows the linear region and the critical region, while only at high $T_\lambda - T$ the Gorter-Mellink region can be seen. The intermediate-diameter capillary, channel II, shows the critical region and the Gorter-Mellink region. The third capillary, channel III, has the largest diameter, and shows the Gorter-Mellink behavior and the onset of critical behavior.

II. APPARATUS

The three channels studied consist of stainless-steel capillaries. The inner diameters are measured by three different methods: (a) by microscope, (b) from the Poiseuille flow of helium gas at room temperature, and (c) from the heat-transport data in the London-Zilsel region. The results are shown in Table I.

The experimental arrangement is shown in Fig. 1. The counterflow tube forms the connection between two reservoirs. The top reservoir has a weak thermal contact with the main helium-bath space by means of an obstructed tube. Thermometers T1, T2, and T3 are modified Allen and Bradley carbon resistors ($R = 220\ \Omega$) mounted on platforms which are soldered to the tube. Thermometers T1 and T2 form the branches of an ac bridge circuit

TABLE I. Diameter determination of the three stainless-steel capillaries and distance between thermometers T1 and T2. The footnotes detail the methods used to measure the inner diameters (i.d.).

Channel	Nominal diameter (mm)	Measured i.d. (mm)	Distance T1-T2 (mm)
I	0.125	0.137±0.004[a] 0.136±0.002[b]	19.0±0.5
II	0.25	0.280±0.005[b]	18.6±0.5
III	0.8	0.80±0.01[c]	16.0±0.5

[a]Thermal conductivity in the London-Zilsel region.
[b]Gas flow at room temperature.
[c]Microscopic observation.

which measures the ratio R_{T1}/R_{T2} and enables us to monitor the temperature difference along the tube while minimizing the influence of the well-known drift in carbon thermometers[6] and of the bath temperature instabilities.

The temperature stabilization is realized in two stages. The temperature of the main bath is controlled by pumping the main bath via an electrodynamic regulating valve.[7] This valve reacts to an error signal of a precision quartz manometer.[8] This combination allows us to stabilize the temperature of the main bath to a precision of 20 μK. Heater H3 and thermometer T3 give additional electronic temperature regulation of the top reservoir. This additional regulation, combined with the above-mentioned resistance ratio bridge allows us to measure temperature differences of less than a μK.

Heat currents along the tube are generated by heater H1. When heater H1 is switched off the electric current is transferred to the identical heater H2 at the other end of the tube. In this way the heat load to the top reservoir and the main bath is constant, greatly facilitating the thermal stabilization of the system.

During precooling the thermal contact of the lower reservoir to the helium bath is very weak. Therefore an additional contact is made via a graphite rod, which acts as a thermal switch because it exhibits a good thermal conductivity around liquid-N_2 temperatures, but a negligible one at liquid-He temperature.

III. EXPERIMENT

An example of an experimental run is given in Fig. 2. Keeping T3 constant the heat current is increased in steps. Between the steps the heat current is set to zero. Thus a certain heat current is always preceded by a zero heat current. As a result the thermal history of the sample is simple and reproducible. (Only occasionally, to check for the presence of hysteresis, is a measuring point approached from the high-heat-current side. However, no hysteresis was found.) The results for the three channels are shown in Figs. 3—5.

Extremely long time constants are sometimes observed. Times as long as several minutes are needed in order to reach equilibrium after the thermal current is switched on (Fig. 2). In some cases times even as long as 20 min are measured.

IV. RESULTS

From the collected data (Figs. 3—5) we can conclude that the heat transport of He II in the counterflow configuration shows three different regions. At low and high heat-current densities one has the London-Zilsel region and the Gorter-Mellink region, respectively. In between one has a transition region which is the most dominant in

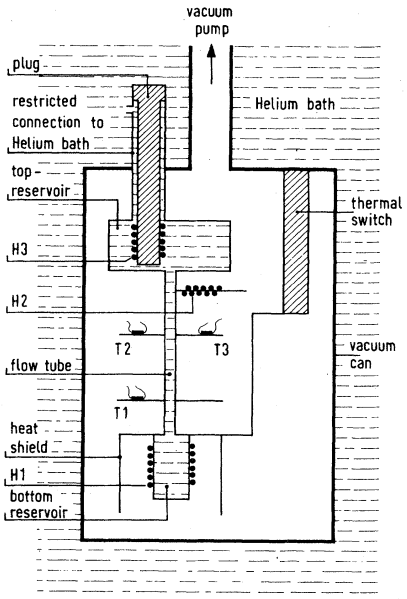

FIG. 1. Schematic drawing of the counterflow arrangement. H1, H2, and H3 are heaters; T1, T2, and T3 are thermometers.

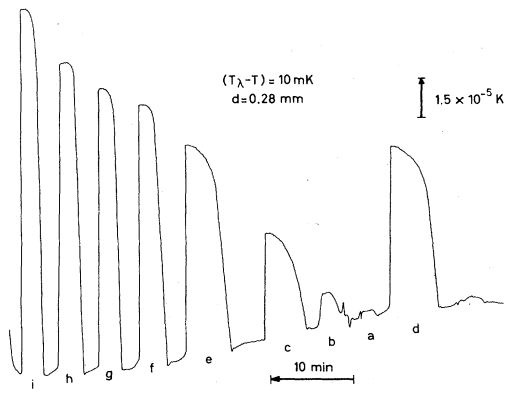

FIG. 2. Example of a recorder output representing an experimental run obtained with a $d=0.28$ mm channel at a temperature $T_\lambda - T = 10$ mK. The ratio R_{T1}/R_{T2} of the two resistance thermometers along the channel is recorded while different heat currents are set. From this ratio the temperature differences can be calculated. The letters under the recorder trace correspond to the letters in Fig. 4. By comparing Fig. 2 with 4 it can be seen that the long response times are only observed in the transition region.

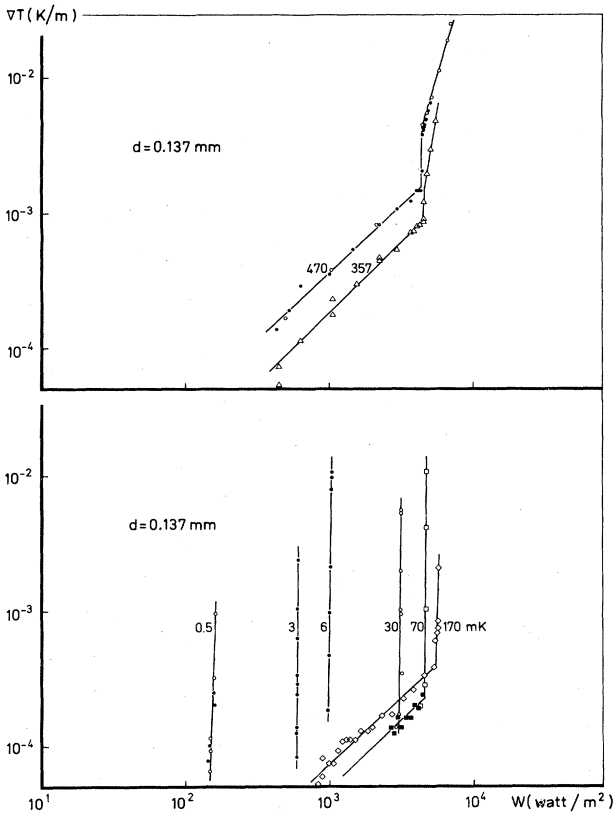

FIG. 3. Logarithmic graphs of collected temperature-gradient (∇T) data as a function of the heat-current density (W) at different temperatures presented by the $T_\lambda - T$ value for a channel diameter $d = 0.137$ mm. When two runs were taken at one value of $T_\lambda - T$, the different runs are indicated by open and solid symbols. The straight lines are to guide the eyes.

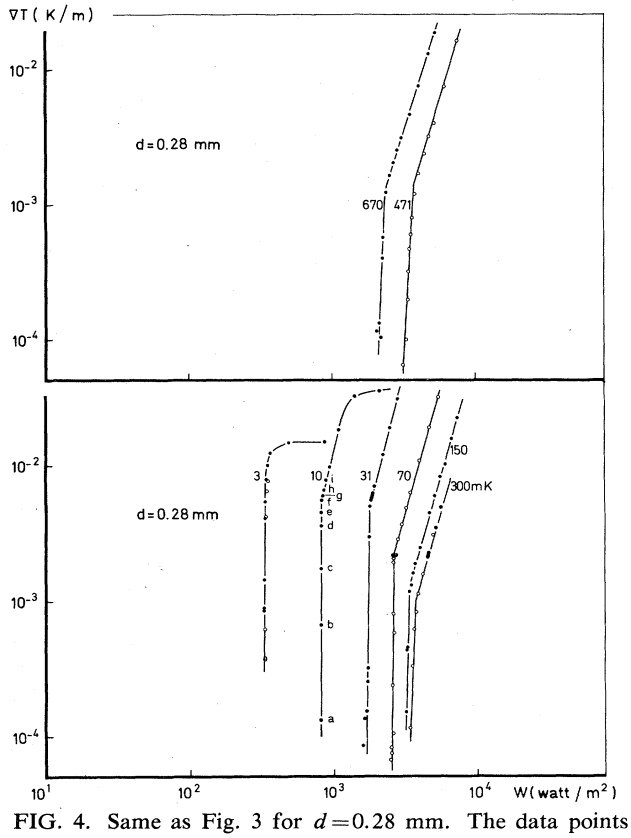

FIG. 4. Same as Fig. 3 for $d = 0.28$ mm. The data points with a letter correspond to the recorder trace given in Fig. 2.

our experimental situation. The existence of this transition region was already noted in the measurements of Brewer and Edwards,[9] of Chase,[10] and of Childers and Tough.[11] The transition region is bounded by two well-defined threshold heat-current densities. Because of the very steep slope of the transition region (Figs. 3—5), both threshold heat-current densities differ only slightly. Therefore we can identify both with the critical-heat-current density W_c. The W_c so found is shown in Fig. 6.

As shown in Fig. 3 a linear region is observed in channel I only at low temperatures.

The Gorter-Mellink region is observed for all three channel diameters. By fitting the data points in this region with expression (2), the values of m are determined. As is also observed in Ref. 3, the exponent m increases with increasing temperature (Fig. 7).

V. DISCUSSIONS

A. Linear region

Only in channel I has a linear region been observed (see Fig. 3). To verify if the linear region corresponds to the London-Zilsel region, we calculate the channel diameter from the thermal-conductivity data, using Eq. (1), and compare the result with the diameter found from a helium-gas-flow measurement at room temperature. The results, $d = (0.137 \pm 0.004)$ mm from the thermal data of He II and $d = (0.136 \pm 0.002)$ mm from the gas-flow measurements, agree very well.

B. The Gorter-Mellink region

One method of verifying the consistency of the measurements on the different capillaries is to study the quotient $W/\nabla T$ at a given ∇T.[12] According to Eq. (2) this should result in a plot independent of the channel diameter as A is expected to be diameter independent.[11,13–15] Figure 8 shows that there is indeed good consistency for

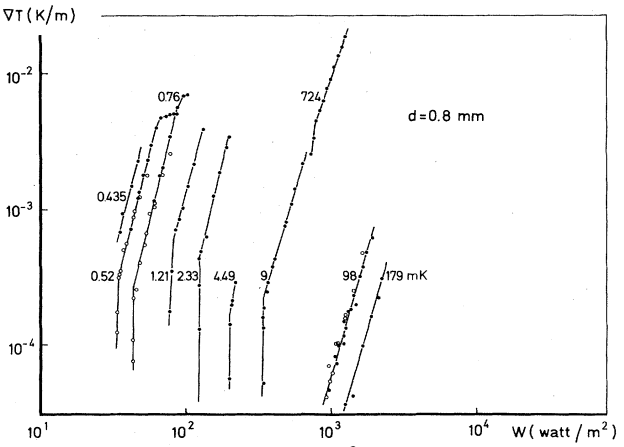

FIG. 5. Same as Fig. 3 for $d = 0.80$ mm.

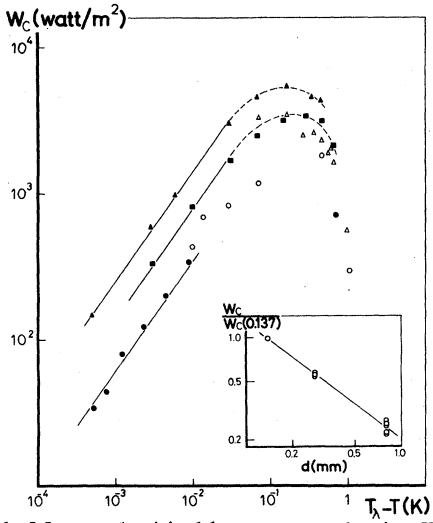

FIG. 6. Measured critical-heat-current density W_c as a function of $T_\lambda - T$. Solid triangles—channel I, $d=0.137$ mm; solid squares—channel II, $d=0.28$ mm; solid circles—channel III, $d=0.80$ mm. Open triangles represent results obtained by Childers and Tough (Ref. 11) on a $d=0.129$ mm glass channel and open circles represent results obtained by Chase (Ref. 10) on a $d=0.80$ mm stainless-steel channel. The solid lines are parallel lines fitted by a least-mean-squares method to the data points below $T_\lambda - T=0.05$ K; the dashed lines are to guide the eyes only. The inset shows the critical-heat-current density W_c relative to the critical-heat-current density of the smallest channel, vs channel diameter. The solid line is a least-mean-squares fit to the data points and shows the exponential dependence $W_c \propto d^{-0.80}$.

the different channel diameters.

To compare our results with the published data of many authors we proceed as follows: Soloski and Frederking[14] derived, from a dimensional analysis, a general expression relating W and ∇T:

$$W = K\rho_s S T \left[\frac{\rho_s}{\rho_n} S \nabla T \eta/\rho\right]^{1/3} . \tag{4}$$

This expression contains only one parameter, K, which Soloski and Frederking fitted to published experimental

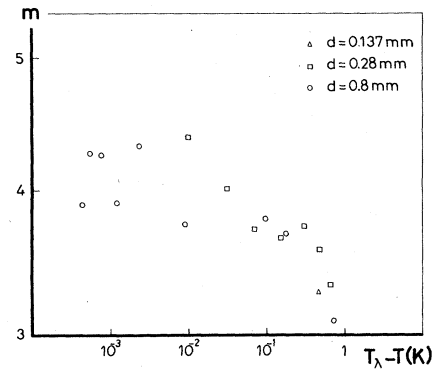

FIG. 7. Exponent m of the generalized Gorter-Mellink equation as a function of $T_\lambda - T$ deduced from the experimental results.

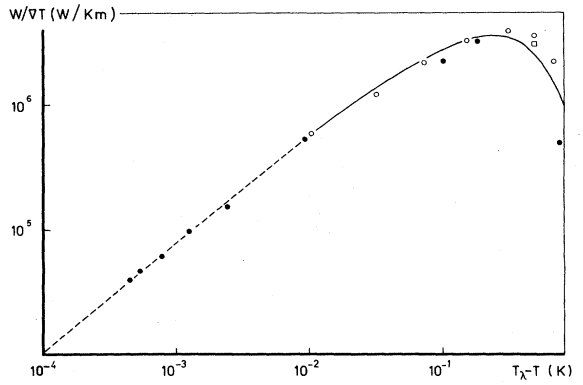

FIG. 8. Quotient $W/\nabla T$ at supercritical-heat-current density ($W > W_c$) as a function of $T_\lambda - T$. This quotient is calculated (if necessary, by means of extrapolation) from experimental results shown in Figs. 3–5, taking a fixed temperature gradient of $\nabla T = 10^{-3}$ K/m. The symbols represent measurements as follows: solid circles, $d=0.80$ mm; open circles, $d=0.28$ mm; one open square, $d=0.137$ mm. The solid-dashed line represents the result from Eq. (4) (see text). Note that this quotient is independent of channel diameter.

results. It was found that the results of many authors covering orders of magnitude of $T_\lambda - T$ will give a value of K equal to 11.3 in Eq. (4), with a variation of approximately $\pm 35\%$. The solid-dashed line in Fig. 8 represents this relation, but with $K=15.1$. The solid part of the line indicates the temperature range used in Ref. 14 to determine K by comparison with the existing data. Our results show that there is also excellent agreement much closer to T_λ (dashed part).

For the limit $T_\lambda - T \to 0$ one can write, for ρ_s,[16]

$$\rho_s = 210 \times (T_\lambda - T)^{2/3} \text{kg/m}^3 , \tag{5}$$

and Eq. (4) can be simplified to

$$W = cK(T_\lambda - T)^{8/9} (\nabla T)^{1/3} . \tag{6}$$

Using[17–19] $S(T_\lambda)=1570$ J/kg K, $\eta(T_\lambda)=24\times10^{-7}$ kg m^{-1} s^{-1}, and $\rho(T_\lambda)=146$ kg/m^3, c has the value 24.1 m$^{1/3}$ K$^{-11/9}$. Indeed, our data closely follow expression (6), as can be seen in Fig. 8 when K is taken to be 15.1. A least-mean-squares fit to the points with $(T_\lambda - T) < 10^{-2}$ K gives an exponent of 0.85, which compares well with the value $\frac{8}{9}$ that followed from the analysis discussed above.

C. Critical region

The observed critical-heat-current densities are plotted in Fig. 6. At somewhat higher $T_\lambda - T$ there exist many earlier determinations of W_c. For illustration, we show results of Childers and Tough[11] on a $d=0.129$ mm channel and of Chase[10] on a $d=0.80$ mm channel. A maximum in W_c is generally observed around 2.0 K, e.g., Refs. 10 and 20.

At low $T_\lambda - T$ the measured points fall reasonably well on three parallel lines, indicating a power-law dependence: $W_c \propto (T_\lambda - T)^\beta$. By means of a least-mean-squares–fit procedure, we fitted three parallel lines through the data points below $T_\lambda - T = 0.05$ K, shown in Fig. 6 as solid

lines. For the exponent β we find a value of 0.75 ± 0.05.

An interesting point is to use our β value to determine the critical velocity v_{sc} in the limit of $T_\lambda - T \to 0$: Using Eqs. (3) and (5) it follows that $v_{sc} \propto (T_\lambda - T)^{-2/3+\beta}$. Inserting the value $\beta=0.75$ gives a v_{sc} value which is weakly decreasing upon approaching T_λ. Indeed, no strong temperature dependence is expected theoretically (for a review, see, e.g., Ref. 21). Measurements of the critical velocity by persistent-current methods also show a nearly-temperature-independent v_{sc} for temperatures close to T_λ.[22] A weak dependence proportional to $(T_\lambda - T)^{1/9}$ is predicted by Jones.[23] The power $\frac{1}{9}$ corresponds to a β value of 0.78, which is in agreement with our result.

The diameter dependence of W_c can also be deduced from Fig. 6. The result is shown in the inset of Fig. 6. The data in this inset were obtained as follows: The measured data points of channels II and III were compared with the corresponding results of channel I by using a linear interpolation between the measured data points of that channel. We find (within the rather limited d range covered by this experiment) a very distinct power-law relation: $W_c \propto d^\nu$, with $\nu=-0.80\pm0.03$. At higher $T_\lambda - T$ one generally finds a similar behavior for W_c with ν equal to about -1 (see, e.g., Ref. 24 and the review in Ref. 21).

As can be seen in Figs. 3–5, the transitions from the London-Zilsel to the Gorter-Mellink regions are extremely steep. It must be emphasized that the slope of the transition region stays finite under all circumstances during our measurements, and that the points in this region in Figs. 3–5 are stable points both when they are reached from the low-W direction as from the high-W direction. Thus we do not observe a discontinuous jump from one region to the other. However, we now mention two mechanisms which, even in the case of a discontinuous change under ideal circumstances, could modify the transition to a more continuous change under the actual experimental conditions. First, the measurements were performed on tubes which were relatively long and, therefore, because of the finite temperature gradient over the tube, one end could reach the critical-heat-current density before the other. However, numerical estimates show that this effect is much too small to explain the observed behavior. Second, because of surface roughness of the channels, there are variations in diameter and, therefore, variations in the heat-current density and W_c, as discussed above. A d variation of 5–10 % can explain the observed slope in the transition region. This variation cannot be excluded for stainless-steel capillaries that are not specially treated. Thus we must conclude that experiments on capillaries specially treated to obtain a constant d are needed to determine unambiguously whether the observed slope is due to imperfect capillaries or to more intrinsic causes related to the nature of the turbulent state.

As is visible in Fig. 2, very long characteristic times are observed. The response time is much longer than the calculated thermal relaxation time of the system formed by the capillary and the hot-end reservoir. Another observed aspect of the behavior in time can also be seen in Fig. 2: Switching off the heat flow results in an immediate collapse of the thermal gradient. The time constants we observed had the following characteristics: (i) It was clearly observed that the long times were noticed only in the transition region. An example can be seen in Fig. 2, where it is shown that the response times became smaller only at the heat flow on the border of the transition and Gorter-Mellink regions. (ii) The times became longer for temperatures close to T_λ. (iii) The response times were longest for the narrowest capillary. (In capillary I we did not observe this effect at all because the response was masked by the long characteristic times of the electronic temperature control that we had to use for that particular measurement.) Especially the above-mentioned difference between switch-on and switch-off behavior suggests that we are seeing the buildup of thermal resistance due to slowly increasing turbulence. Similar effects (although for much shorter time constants) have been studied in a more direct way by Vinen.[25] In his experiment the turbulence was observed by means of second-sound absorption.

Chase[10] and Ladner *et al.*[26] also observed effects which were similar in thermal counterflow experiments. These authors also observed that the times are largest around the critical heat flow.

Figure 9 shows schematically how the measurements of the decay times were performed. Switching off the heat flow for a short time and then switching it on brings the temperature gradient nearly back to the value it had immediately prior to switching off. Increasing the time in the switched-off state in a systematic way allows one to measure the decay time. In the present experiment, however, we have studied this only qualitatively, and in accordance with Vinen[25] we find that the decay time is shorter than the buildup time.

A final point we would like to discuss is the nature of the observed transition. It has been noted that different critical-heat-current densities can be observed. Especially in tubes with a round cross section this effect is very pronounced. An excellent review on this phenomenon was written by Tough.[15] In it he notes that for round tubes two types of critical-heat-current densities are found: type I, the lowest critical-heat-current density, separates the linear region from a turbulent region, while type II separates the above-mentioned turbulent region from a turbulent region of a different (but unknown) nature. Because in most of our experiments the linear region is not observed, we cannot ascertain with certainty which type

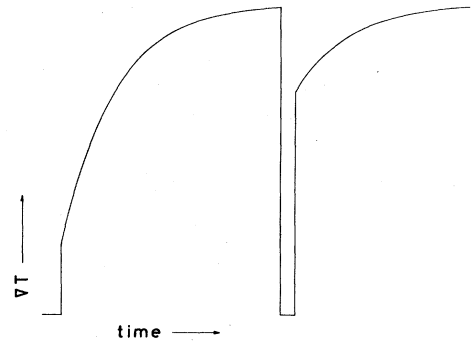

FIG. 9. Schematic drawing of a recorder trace of an experiment aimed at the determination of the thermal resistance decay.

of transition is manifested. However, Tough[15] argues that when the circumstances are such that the normal fluid is not turbulent, a type-I transition is observed. Reasoning along these lines it seems plausible that in our case, for the observations close to T_λ where the normal fluid has a very low velocity, the transition is of type I. Also, the v_{sc} that we observe around 2 K ($v_{sc}d \simeq 4\times10^{-6}$ m^2/sec at 2.0 K and $v_{sc}d \simeq 3\times10^{-6}$ m^2/sec at 1.9 K) agrees well with the values observed for a type-I transition (compare with Figs. 39 and 40 of Ref. 15). On the other hand, a type-I transition is usually accompanied by hysteresis phenomena which we do not observe.

VI. CONCLUSIONS

In the regions where other experiments are available for comparison, we find generally good agreement. In the temperature region close to T_λ, the results obtained turn out to show simple relationships. The heat-current density in the Gorter-Mellink region is proportional to $(T_\lambda - T)^{0.85}$, in close agreement with the expectation based on a dimensional analysis in which a value of $\frac{8}{9}$ for the exponent was expected. The critical-heat-current density W_c is proportional to $(T_\lambda - T)^\beta$, with $\beta = 0.75 \pm 0.05$. From this value of β it follows that the critical velocity v_{sc} is weakly dependent on $T_\lambda - T$: $v_{sc} \propto (T_\lambda - T)^{0.08\pm0.05}$. A weak temperature dependence has also been observed at lower temperatures and is also expected close to T_λ. For example, an exponent of $\frac{1}{9}$ has been predicted,[23] in agreement with what we found. The diameter dependence of W_c obeys very well the exponential law $W_c \propto d^\nu$, with $\nu = -0.80 \pm 0.03$.

A striking phenomenon observed during our experiment was the presence of extremely long relaxation times. More systematic research could possibly give useful information on the buildup of the turbulence in the critical region. Also, the steepness of W versus ∇T is quite striking. Further investigation is needed on different types of capillaries to find out whether this aspect of the critical behavior has to do with the properties of the capillaries or is intrinsic to the buildup of turbulence in the temperature range close to T_λ.

ACKNOWLEDGMENTS

We thank Dr. H. W. Myron for a careful reading of the manuscript. Part of this work was supported by the Stichting voor Fundamenteel Onderzoek der Materie (FOM) with financial support from the Nederlandse Organisatie voor Zuiver Wetenschappelijk Onderzoek (ZWO). One of the authors (T.H.K.F.) acknowledges partial support from the National Science Foundation (NSF) under Grant No. CPE-81-05153.

*Present address: Rijksakademie Nieuw Rollecate, 7415 CR Deventer, The Netherlands.

[1]F. London and P. R. Zilsel Phys. Rev. **74**, 1148 (1948).
[2]C. J. Gorter and J. H. Mellink, Physica (Utrecht) **15**, 285 (1949).
[3]M. J. Crooks and D. L. Johnson, Can. J. Phys. **49**, 1035 (1970).
[4]W. F. Vinen, Proc. R. Soc. London, Ser. A **242**, 493 (1957).
[5]K. W. Schwarz, Phys. Rev. B **18**, 245 (1978).
[6]W. L. Johnson and A. C. Anderson, Rev. Sci. Instrum. **42**, 1296 (1971).
[7]Electrodynamic valve model NW 10 KF and Elektronisches Regelgerät model ER 3, Leybold-Heraeus GmbH, Köln, West Germany.
[8]Mensor Quartz-Manometer, Mensor Corporation, San Marco, Texas 78666.
[9]D. F. Brewer and D. O. Edwards, Philos. Mag. **6**, 775 (1961).
[10]C. E. Chase, Phys. Rev. **127**, 361 (1962).
[11]R. K. Childers and J. T. Tough, Phys. Rev. B **13**, 1040 (1976).
[12]W. H. Keesom, B. F. Saris, and L. Meyer, Physica (Utrecht) **7**, 817 (1940).
[13]P. E. Dimotakis and J. E. Broadwell, Phys. Fluids **16**, 1787 (1973).
[14]S. C. Soloski and T. H. K. Frederking, Int. J. Heat Mass Trans. **23**, 437 (1980).
[15]J. T. Tough, in *Progress in Low Temperature Physics,* edited by D. F. Brewer (North-Holland, Amsterdam, 1982), Vol. VIII.
[16]J. R. Clow and J. D. Reppy, Phys. Rev. Lett. **16**, 887 (1966); D. S. Greywall and G. Ahlers, Phys. Rev. A **7**, 2145 (1973).
[17]C. J. N. van den Meijdenberg, K. W. Taconis, and R. de Bruyn Ouboter, Physica (Utrecht) **27**, 197 (1961).
[18]F. A. Staas, K. W. Taconis, and W. M. van Alphen, Physica (Utrecht) **27**, 893 (1961).
[19]E. C. Kerr and R. D. Taylor, Ann. Phys. (Leipzig) **20**, 450 (1962).
[20]S. G. Hegde and W. I. Glaberson, Phys. Rev. B **24**, 2474 (1981).
[21]V. Arp, Cryogenics **10**, 96 (1970).
[22]J. R. Clow and J. D. Reppy, Phys. Rev. Lett. **19**, 291 (1967).
[23]B. K. Jones, Phys. Rev. **177**, 292 (1969).
[24]D. R. Ladner and J. T. Tough, Phys. Rev. B **20**, 2690 (1979).
[25]W. F. Vinen, Proc. R. Soc. London, Ser. A **240**, 128 (1957).
[26]D. R. Ladner, R. K. Childers, and J. T. Tough, Phys. Rev. B **13**, 2918 (1976).